Gan, W.M.; Huang, Y.D.; Wang, R.; Wang, G.F.; Srinivasan, A.;
Brokmeier, H.-G.; Schell, N.; Kainer, K.U.; Hort, N.:

Microstructures and mechanical properties of pure Mg processed by rotary swaging

In: Materials and Design (2014) Elsevier

DOI: 10.1016/j.matdes.2014.05.057

Microstructures and mechanical properties of pure Mg processed by rotary swaging

W.M. Gan [a, #], Y.D. Huang [a, *, #], R. Wang [b, #], G. F. Wang [c, #], A. Srinivasan [d, #], N. Schell [a], K.U. Kainer [a], N. Hort [a]

[a] Institute of Materials Research, Helmholtz-Zentrum Geesthacht, Max-Planck-Str. 01, D-21502 Geesthacht, Germany

[b]Institute for Materials Science and Engineering, Clausthal University of Technology, Clausthal-Zellerfeld Germany

[c]Wenzhou Medical College, Affiliated Taizhou Hospital, Luqiao Division, Taizhou City 318050, Zhejiang Province, China

[d]National Institute for Interdisciplinary Science and Technology, CSIR, Pappanamcode (P.O), Thiruvananthapuram 695 019, India

*Corresponding author: yuanding.huang@hzg.de; Tel. +49-4152871935; Fax: +49-4152871909

# These authors contributed equally to this paper.

Abstract

Microstructures and tensile properties of commercial pure magnesium processed by rotary swaging (RS) technique were investigated. Bulk and gradient textures in the RS processed Mg were characterised by neutron and synchrotron diffractions, respectively. Grains of the pure Mg were gradually refined with increase in the RS passes, which largely contributed to an increase in the tensile yield strength. A dominated basal fibre texture was observed in the RS processed pure Mg. Accommodated twinning deformation was also observed. Both the optical observations and texture analyses through the diameter showed a gradient evolution in microstructure.

Keywords: swaging, magnesium, microstructure, tensile property

1. Introduction

Swaging is a forging process in which the dimensions of an item are altered using a die or dies by applying force. It is usually a cold working process; however, it also can be a hot working process.

Rotary swaging is primarily suitable for cylindrical parts made from rods, tubes, and wires [1, 2]. The low tooling cost and fast setup make swaging an economical process for the production of even hundreds of pieces. The high output rate and material savings often make it also suitable for the highest production applications. Swaging process is widely used to make Al alloys, steel and Cu alloys products but not extensively used for Mg and its alloys till nowadays [2-4].

Mg and its alloys are one of the lightest structural materials. However, they have relatively low strength and ductility which limits their applications. Efforts have been taken to improve the mechanical properties of Mg by alloying and microstructural optimization by mechanical deformations [5, 6].

Conventional rolling and extrusion on Mg can help to improve the tensile properties, but the deformed Mg always exhibits a high strong anisotropy [7, 8]. Recent investigations on severe plastic deformations (SPD), such as equal channel angular pressing (ECAP) and high pressure torsion (HPT) of Mg and its alloys have been widely performed [6, 9]. Results showed that the SPD processed Mg alloys demonstrated a high ductility but relatively low strength [7]. Due to the limitation of deformation conditions the large scaled application of previous SPD techniques on Mg and its alloys is still in progress [10]. Swaging deformation on Mg and its alloys has not been so far widely carried out even though it is a traditional forming technology.

Mg easily appears anisotropy because of its intrinsic HCP (Hexagonal close-packed) crystallography structure which has limited slip systems at low temperatures [11]. Texture development of Mg alloys by conventional thermomechanical processes such as hot extrusion, forging, and rolling are well understood [8, 12]; and as well their anisotropic tensile or compression stress-strain behaviours [13]. Basal plane sliding accommodated by twinning deformation was mainly considered to be the formation of preferred orientation/ texture in Mg. Unique texture developed via ECAP/ECAE (equal channel angular extrusion) has widely been investigated in the last years by experimental and as well by the simulation [6, 7, 14, 15]. During ECAP/ECAE processing the basal planes gradually orientating normal to the shear direction via different

processing routes were reported. This was also proved by the texture gradient analysis in ECAP processed pure Mg [16]. A stationary oblique B fibre which is a typical simple shear deformation has been reported in HPT processed pure Mg [9, 17]. Few investigations were carried out to explore the texture development during swaging of Mg [18, 19]. Moreover, most of them did not systematically clarify the bulk texture evolution and as well the texture distribution.

Current investigations were undertaken to study first the microstructure and texture (bulk and local) of the RS processed pure Mg. Their evolutions will be related to the RS deformation mechanism. Second, the tensile properties at room temperature of the RS processed pure Mg will be investigated and discussed.

2. Experimental

Rods of diameter of 10 mm and height of 100 mm machined from the commercial pure Mg (99.99%, Xinxiang Jiuli Magnesium Co., Ltd, China) ingots were used as raw materials [Fig. 1 (a)]. A stationary spindle swaging machine was from Heinrich Müller. The principle of its operation was illustrated in Fig. 1 (b); and as well as the sample coordinate definition (SD- swaging direction, R- radial direction, H- hoop direction). The rod sample was heated to a desired temperature and held for 10 minutes before each swaging deformation. The heating temperature selected was gradually decreased (Fig. 2). Sample S7 was swaged out at room temperature. A set of molds was used to reduce the size of work piece from Ø 10 mm to Ø 4.5 mm. Typical deformed samples at different strain levels (marked as S1, S2, ... , S7 in Fig. 2) were selected for the further investigations. The true strain of the samples calculated based on area reduction using the relationship, $\varphi=\ln (A_0/A)$, is listed in Table 1.

The samples for optical investigations were taken from the longitudinal sections of the rods. The samples were firstly cold mounted, and progressively ground with SiC water proof papers up to 2000 grid size. Finally the samples were polished on a rotating disc with 0.05 μm suspended silica (OPS) as abrasive particles with NaOH as lubricant. The polished samples were chemically etched

in a solution of 8 g picric acid, 5 ml acetic acid, 10 ml distilled water and 100 ml ethanol. They were observed under Reichert-Jung MeF3 optical-microscope attached with analySIS pro software.

Bulk texture evolution of the swaged samples was measured using the thermal neutron diffractometer STRESS-SPEC located at the FRM II, Heinz Maier-Leibniz Zentrum (MLZ) Garching, Germany [20]. Samples with a height of 10 mm machined from the swaged were used for the texture measurements. Five pole figures were measured using two detector positions with a wavelength of 0.164 nm. These 5 pole figures were used to calculate the orientation distribution function (ODF) using series expansion method with an expansion degree of l_{max}= 22 and to recalculate pole figures as well as ODF sections from ODFs [21]. Texture gradient from the surface to the center of the rod was analysed using synchrotron radiation at HEMS - High Energy Materials Science Beam line P07 at PETRA III, DESY Germany. The beam size was 50 μm×50 μm. The detail of the measured positions will be shown in the following section.

Tensile tests were carried out at room temperature using an Instron 5569 universal testing machine at an initial crosshead speed of 1 mm·min^{-1}. The tensile axis was parallel to the swaging direction (SD as marked in Fig. 1 (b)) of the rod.

3. Results

3.1 Microstructures

Fig. 3 shows the optical microstructures of the samples S1 to S7. Coarse grains with an average size of about 4.5 mm were observed in the as-cast pure Mg. After swaging processing with 2 cycles (S2) the grain was refined with a bimodal distribution, i.e. some large grains about 120 μm were surrounded by small grains about 40 μm in an average diameter. Many twins inside the large grains were clearly observed. In the sample S3, large grains of about 50 μm surrounded by small grains of 25 μm were observed. The grain size of S4 was uniformly refined to about 30 μm with no existence of the large grains. Both the samples S6 and S7 have an average grain size of about 25 μm.

Detailed microstructure observations of the sample S7 on the plane which was parallel to the SD direction (rod feeding) were performed. The results are shown in Fig. 4. The high magnification

micrographs of the regions marked as A, B and C are also presented in Fig. 4. Position A, which is near the surface of the rod, shows many shear bands like appearance. These shear bands were remained to some degree at position B also. At position C, no shear bands were seen and the grains were mostly recrystallized. Moreover, the grain size decreased from the surface to the centre. It should be mentioned that such kind of distribution of the microstructures is a typical phenomenon in swaging process, indicating that there should be an inhomogeneous deformation occurs from the surface to centre of rod during swaging [3, 4]. Therefore, a local texture analysis was performed to further characterize the swaging deformation. The results will be discussed in the next section.

3.2 Textures

3.2.1 Bulk texture evolution

Fig. 5 shows the texture evolution of the samples of S2 to S7 using the ODF-sections PHI2=0° and 30°, respectively. There exists a main {00.1} basal fibre at the first stage for the sample S2, which is similar to the texture of typical hot compression or forging of Mg [11]. In between two weak components {10.0} and {11.0}, the prismatic planes were also observed. These two components should come from the reheat treatment. These prismatic planes slip should also be accommodated by the compression twinning because the basal planes are already re-orientated for the input of S2.

For the sample S3, which was 4 times swaged after S2, the maximum intensity in ODFs increased. It still showed a basal fibre but with an increase of another two prismatic plane components. This should be attributed to the recrystallization effect. The {00.1} basal plane intensity increased with sample S4 which was one time swaged after S3. The sample S6 exhibited a little higher maximum basal intensity than that of S5. For the sample S7 which had the same diameter as that of the sample S6 but swaged at room temperature the maximum intensity in ODFs decreased with the recrystallization component compare to S6. This can be also seen from the optical microstructures.

3.2.2 Texture gradient

The specimen with a dimension of Ø 4.55× 4.55 mm^2 was used for texture gradient measurement by synchrotron radiation. The measured positions A, B and C were similar to those marked in Fig. 4 which represented these locations in the rod near the outer surface, 1 mm to the outer surface and at the centre, respectively. The (10.0) and (00.2) pole figures of the local texture analysis at these corresponding positions for the sample S7 are shown in Fig. 6, respectively. In general, at all the positions strong basal fibre was observed. However, at the positions A and B the basal planes in some grains were orientated about 45° to the R-direction; and two symmetric axes marked in dashed lines can be clearly seen at position B. This re-orientation of the basal plans was much more obvious at the position A. According to the microstructures shown in Fig. 4 both the positions A and B have shearing bands.

3.3 Tensile property

The tensile yield strength (TYS) and the tensile elongation of the samples S1 to S7 are shown in Fig. 7 (a) and (b), respectively. The TYS of two times swaged sample (S2) increased marginally compared to that of the as-cast sample (S1): the increase was from 53 MPa to 60 MPa. The TYS was monotonously increased. The TYS of sample S7 was 3 times higher than that of the as-cast sample. After swaged 4 times the increase of TYS was slowed down and it tended to be stable. Similar result was reported by Abdulstaar *et al.* They investigated the evolution of yield stress of pure aluminium with swaging cycles; and observed a saturation plateau on the curve (TYS as a function of swaging cycle) [3].

However, the tensile elongation curve showed a different variation (Fig. 7 (b)). The elongation increased about 4 times from that of the as-cast to that of S2 and S3; then decreased to about 2 % with S4 to S7. Actually, distribution of the tensile elongation of samples S4 to S7 was around this value, which might indicate a saturated platform of the ductility of the RS processed Mg.

4. Discussions

From the above description the bulk texture development shows a strong relationship with the RS process pass. In principle the swaging deformation looks like a multiple directional forging plus

extrusion of a rod. The grain size of RS processed pure Mg can be greatly refined even with few cycles. Dominant basal planes sliding accommodated by twinning deformation lead to the formation of strong basal fibre texture [11]. Partially recrystallization also occurred due to a relatively high swaging temperature. As the grain size reduced with more swaging cycles, the prismatic planes became activated and hence twinning deformation could be suppressed. However, the dynamic recrystallization always occurred during RS process.

Inhomogeneous distribution of the grain size and texture represented the non-uniform deformation along the diameter from surface to centre of the RS processed rod. Existence of the shear band near the surface should mainly result from the different rod feeding speed at each cycle and the friction between the die and rod. Since the rod was manually fed using the current available swaging machine it was hard to keep a constant and uniform feeding rate. This led to an asymmetric distribution of the basal planes around the SD (marked in Fig. 6). Moreover, the unavoidable temperature gradient from surface to the centre of the rod could also contribute to the microstructural inhomogeneity. However, the degree of inhomogeneity decreased with the increase in the number of swaging process cycle due to lowering the deformation temperature. This was the reason for the gradual reduction in temperature during the present RS experiments (ref. Fig. 2). Moreover, continuously lowering the temperature could also contribute to the stability of microstructure, as reported by the ECAP processed Al-Mg alloy [22]. Texture inhomogeneity or gradient was widely found in ECAP processed pure Mg and copper [16, 23], and as well the HPT process [24]. However，this texture inhomogeneity tended to be alleviated with the increase of process cycle / pass, which is similar to that observed in the current investigation.

Furthermore, evolution of the tensile property is greatly related to the microstructures of the RS processed pure Mg, i. e., grain size and its distribution, and the inner preferred grain orientation. Continuous increase of the TYS with the swaging cycle demonstrated the effectiveness of the swaging process to increase the strength of pure Mg. Gradual increase of the TYS shown in Fig. 7 (a) with the swaging cycle could mainly attribute to the reduction of grain size and the increment of

dislocation density. At a lower temperature or room temperature, only partial recrystallization took place. The saturation of TYS observed at the later stage of swaging suggested that the microstructure was tending to be stable [3]. The changes in the grain size and the dislocation density were not apparent at that time. However, the variation of the tensile elongation showed difference of TYS. Both the S2 and S3 samples demonstrated a rapid increase in ductility from that of the as-cast, which was mainly due to the bimodal distribution of the grains. Similar effect of the bimodal grains on the strain was also reported in sever plastic deformations like ECAP, HPT, and *etc*. [25]. Hence, effective grain refining with the RS process played the important role in improving the tensile properties. The saturation of the grain refinement from S4 to S7 was responsible for the nearly stable corresponding tensile elongation variation (in Table 1).

Finally, it is interestingly noted that the TYS of the swaged S7 (deformation strain of ~1.58) showed a similar value of pure Mg processed with ECAP after 4 passes (deformation strain of ~4) [26]; but the maximum intensity of the basal fibre texture in the present RS processed sample was half of that observed in the ECAP processed pure Mg [16, 27]. This may be due to the different deformation modes of two techniques. Swaging deformation behaves like multi-directional forging while mechanical shearing is the main deformation mode in ECAP [28]. Re-orientation of the basal planes in most grains was different with these two processing modes. Moreover, temperature should also play an important role for the produced texture since it affects the recrystallization during and after deformation. Hence, RS can effectively improve the tensile strength while ECAP is efficient to increase the ductility in comparison with these two studies on Mg.

5. Conclusions

With the rotary swaging proceeding, the grain size of pure magnesium can be effectively refined. The microstructure was inhomogeneous from the surface to the centre of rods due to the existence of shear deformation at the near surface region. A strong {00.1} basal fibre texture was observed. Its maximum intensity slightly increases with increasing the RS process pass. The tensile yield stress monotonously increased and tended to be stable during swaging. The tensile elongation first

increased, reached the maximum at a swaging strain of about 1, and then decreased again with further RS processing. RS processing on pure Mg with less deformation strains is very efficient to increase the tensile strength as compared to ECAP.

References

[1] Grosman F, Piela A. Metal flow in the deformation gap at primary swaging. J of Mater Pros Techno 1996; 56: 404-411.

[2] Lyman T. Forming, Metals handbook 8th ed., Park, Ohio: American Society for Metals; 1969.

[3] Abdulstaar MA, El-Danaf EA, Waluyo NS, Wagner L. Severe plastic deformation of commercial purity aluminum by rotary swaging: Microstructure evolution and mechanical properties. Mater Sci & Eng 2013; A565: 351-358.

[4] Klau PN, Brandaob L, Ortiz F, Egungwu O, Ige F. On the texture evolution in swaged Cu-based wires. Scripta Mater 1998; 38: 1755-1761.

[5] Hort N, Huang YD, Abu Leil T, Maier P, Kainer KU. Microstructural investigations of the Mg-Sn-XCa System. Advan Eng Mater 2006; 8(5) 359-364.

[6] Gan WM, Zheng MY, Chang H, Wang XJ, Qiao XG, Wu K, Schwebke B, Brokmeier HG. Microstructure and tensile property of the ECAPed pure magnesium. J of Alloys & Comp 2009; 470: 256-262.

[7] Brokmeier HG, Gan WM, Zheng MY, Zuberova Z, Estrin Y. Development of extrusion and rolling textures during ECAP of Mg-alloys. Mater Sci Forum 2008; 584-586: 748-753.

[8] Bohlen J, Yi SB, Swiostek J, Letzig D, Brokmeier HG, Kainer KU. Microstructure and texture development during hydrostatic extrusion of magnesium alloy AZ31. Scripta Mater 2005; 53: 259-264.

[9] Harai Y, Kai M, Kaneko K, Horita Z, Langdon TG. Microstructural and Mechanical Characteristics of AZ61 Magnesium Alloy Processed by High-Pressure Torsion. Mater Trans 2008; 49: 76-83.

[10] Zhilyaev AP, Gimazov, AA, Langdon TG. Recent developments in SPD processing of ultrafine-grained metals and alloys. J of Mater Sci 2013; 48 (13): 4461-4466.

[11] Wang YN, Huang JC. Texture analysis in hexagonal materials. Mater Chem & Phy 2003; 81: 11-26.

[12] Wan G, Wu BL, Zhang YD, Sha GY, Esing C. Anisotropy of dynamic behavior of extruded AZ31 magnesium alloy. Mater Sci & Eng 2010; A (527): 2915-2924.

[13] Geng CJ, Wu BL, Du XH, Wang YD, Zhang YD, Wagner F, Esling C. Stress-strain response of textured AZ31B magnesium alloy under uniaxial tension at the different strain rates. Mater Sci & Eng 2013; A (559): 307-313.

[14] Wu BL, Wan G, Zhang YD, Du XH, Wangner F, Esling C. Fragmentation of large grains in AZ31 magnesium alloy during ECAE via route A. Mater Sci & Eng 2010; A (527): 3365-3372.

[15] Agnew S, Mehrotra P, Lilo TM, Stoica GM, Liaw PK. Texture evolution of five wrought magnesium alloys during route A equal channel angular extrusion: Experiments and simulations. Acta Mater 2005; 53 (11): 3135-3146.

[16] Gan WM, Brokmeier HG, Chang H, Zheng MY, Wu K. Texture gradient in a single pass ECAPed pure Mg by neutron radiation. Mater Sci Forum 2008; 584-586: 513-517.

[17] Bonarski BJ, Schafler E, Mingler B, Skrotzki W, Mikulowski B, Zehetbauer MJ. Texture evolution of Mg during high-pressure torsion. J Mater Sci 2008; 43: 7513-7518.

[18] Schwaneke AE, Nash RW. Effect of preferred orientation on damping capacity of magnesium alloys. Metall Trans 1971; 2: 3453- 3457.

[19] Shahzad M, Wagner L. Thermo-mechanical methods for improving fatigue performance of wrought magnesium alloys. Fatigue Fract Eng Mater Struct 2009; 33: 221-226.

[20] Brokmeier HG, Gan WM, Randau C, Voeller M, Rebelo-Kornmeier J, Hofmann M. Texture analysis at neutron diffractometer STRESS-SPEC. Nucl Instr & Meth in Phy Res 2011; A (642): 87-92.

[21] Bunge HJ. The ODF Calculation from Pole Figures for Different Types of Crystal and Sample Symmetries. Mater Sci Forum 1994; 157-162: 401-406.

[22] Yamashita A, Yamaguchi D, Horita Z, Langdon TG. Influence of pressing temperature on microstructural development in equal-channel angular pressing. Mater Sci & Eng 2000; A287: 100-106.

[23] Esling C, Humbert H, Schwarzer RA, Wagner F. Texture gradient in ECAP copper by synchrotron radiation. Solid State Phenon 2005; 105: 327-332.

[24] Alexandrov IV, Zhilina MV, Bonarski JT. Formation of texture inhomogeneity in severely plastically deformed copper. Bull Pol Ac: Tech 2006; 52 (2) 199- 208.

[25] Hoeppel HW, Korn M, Lapovok R, Mughrabi H. Bimodal grain size distributions in UFG materials produced by SPD: Their evolution and effect on mechanical properties. J of Phy Conf Series 2010; 240: 012147.

[26] Gan WM. Texture and Microstructure Development of the Silicon containing Magnesium Alloys after Equal Channel Angular Pressing, doctoral degree thesis: Technical University of Clausthal, Germany, 2008.

[27] Biswas S, Singh DS, Bhowmik A, Suwas S. Study of Texture Evolution of pure magnesium during ECAE using EBSD. Mater Sci Forum 2008; 584-586: 343-348.

[28] Su CW, Lu L, Lai MO. model for the grain refinement mechanism in equal channel angular pressing of Mg alloy from microstructural studies. Mater Sci & Eng 2006; A434: 227-236.

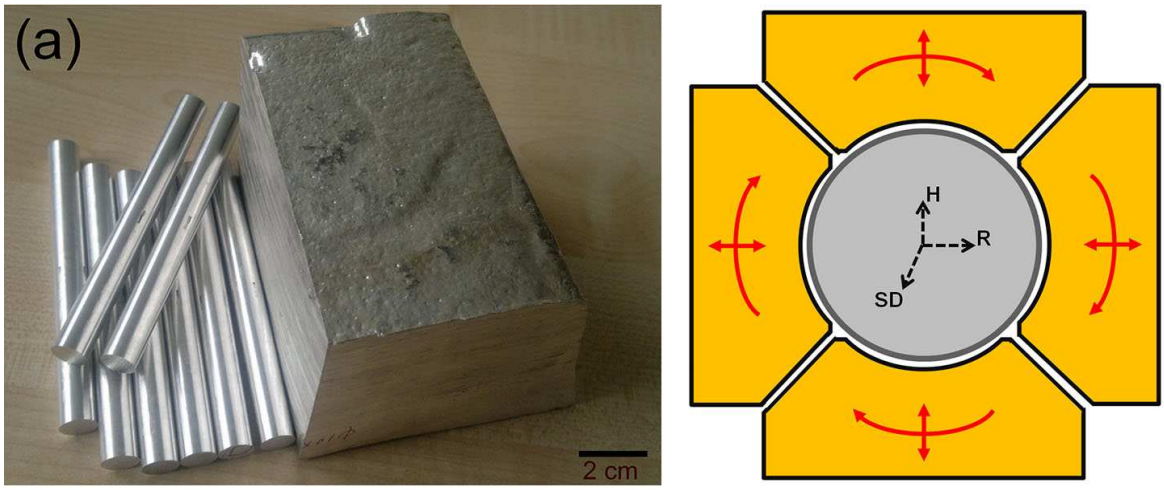

Fig. 1 (a) As-cast pure ingot and the rods for swaging; (b) illustration the principle of operation of the rotary swaging.

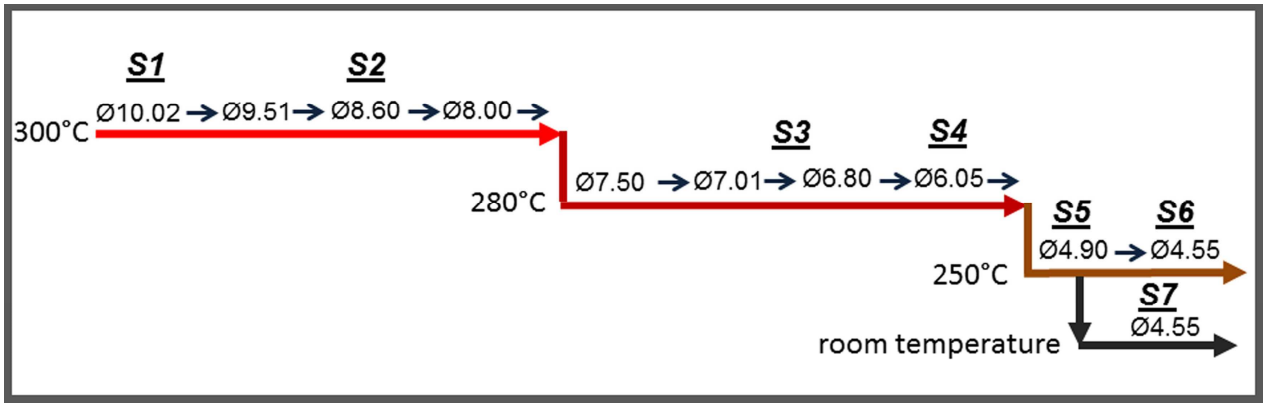

Fig. 2 Schematic diagram for swaging process.

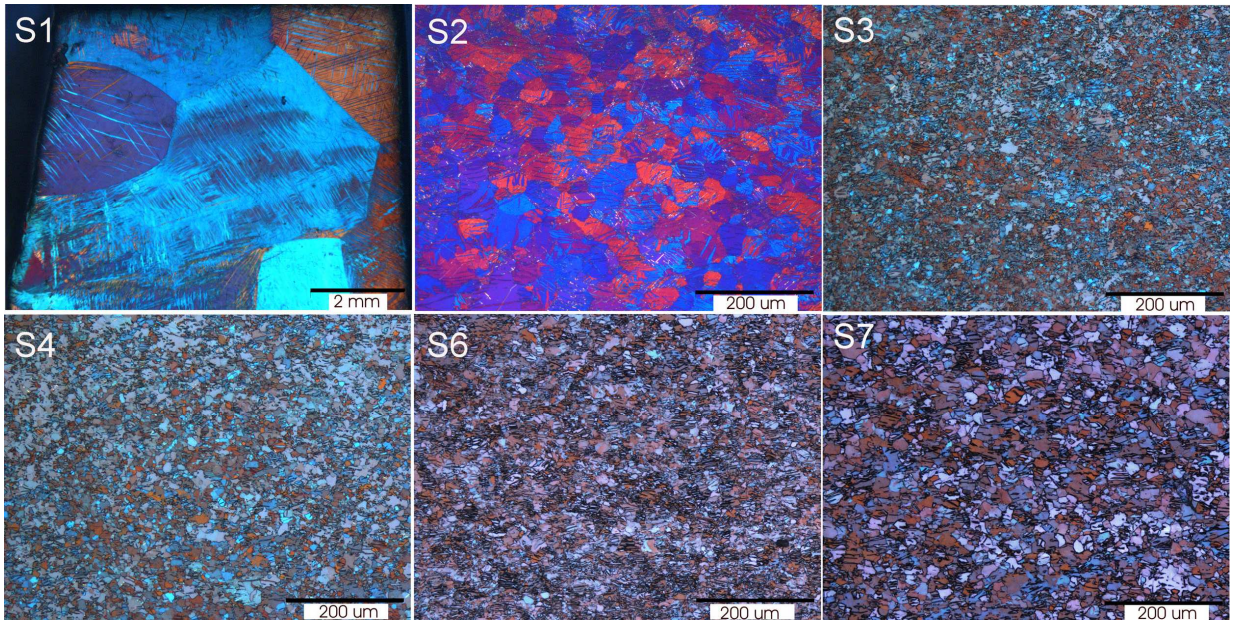

Fig. 3 Optical microstructures of the swaged samples.

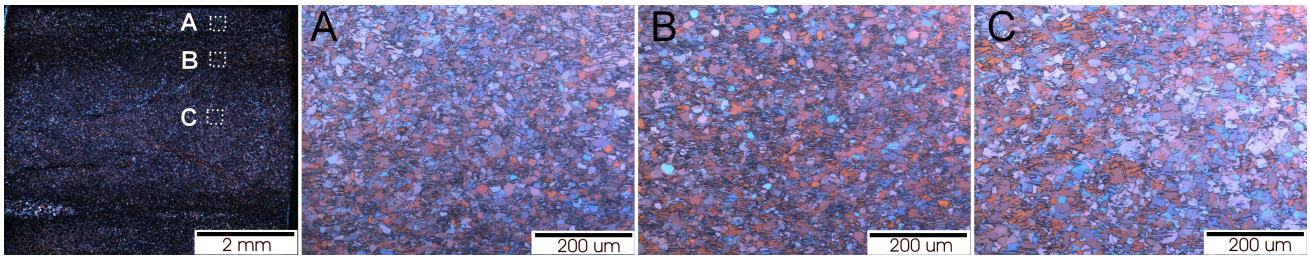

Fig. 4 Optical microstructures at different positions A, B and C of S7 from the surface to center.

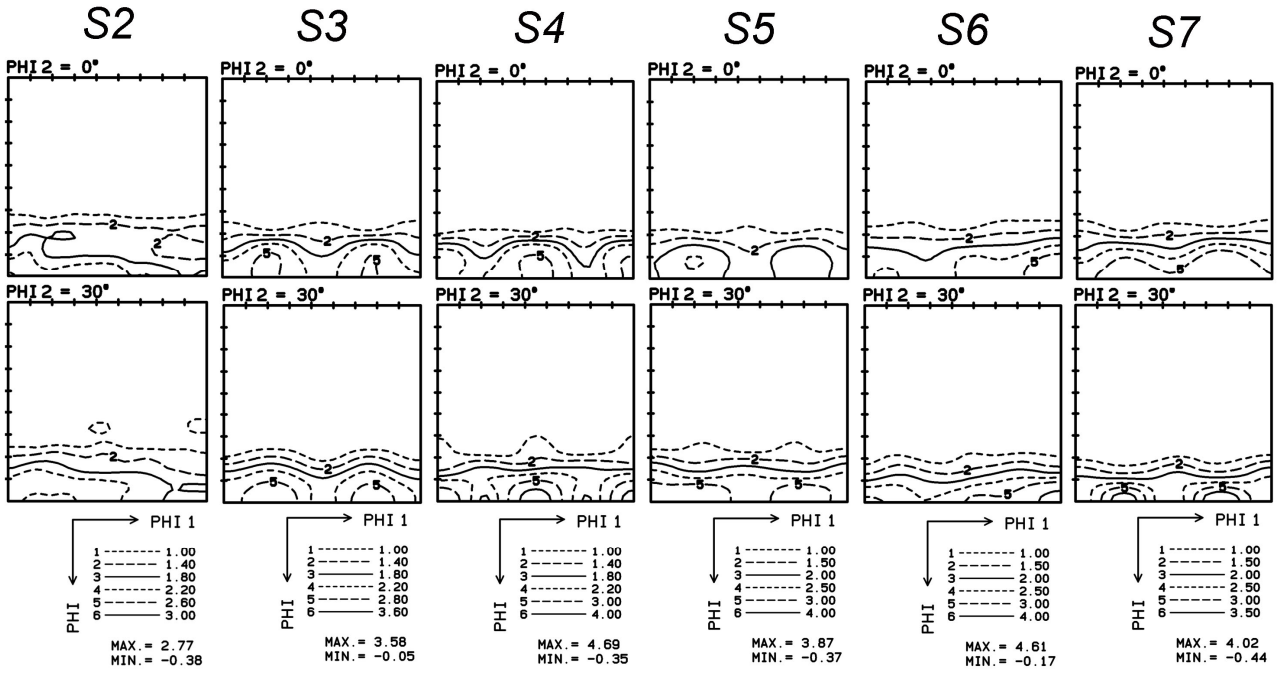

Fig. 5 ODFs evolution at PHI2 sections of 0º and 30º for the samples from S1 to S7.

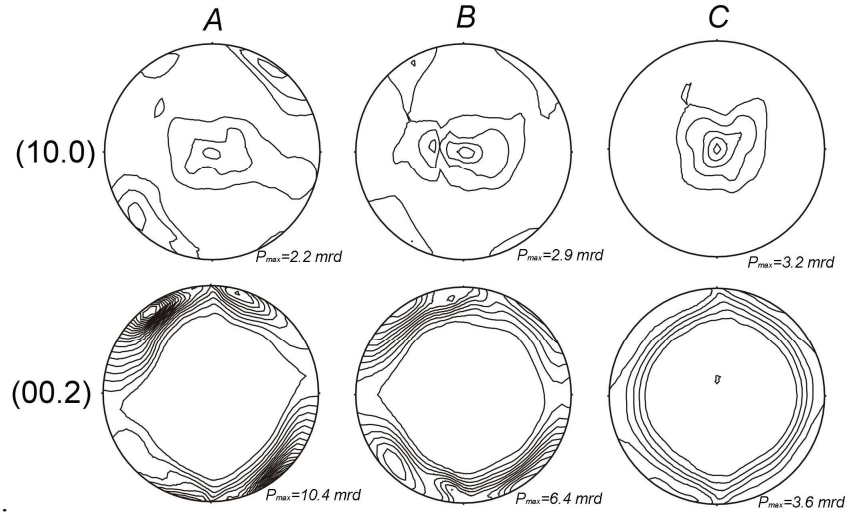

Fig. 6 (10.0) and (00.2) pole figures of sample S7 at positions A, B and C which are marked in Fig. 4, respectively (contour levels=1.0×, 1.5×, …).

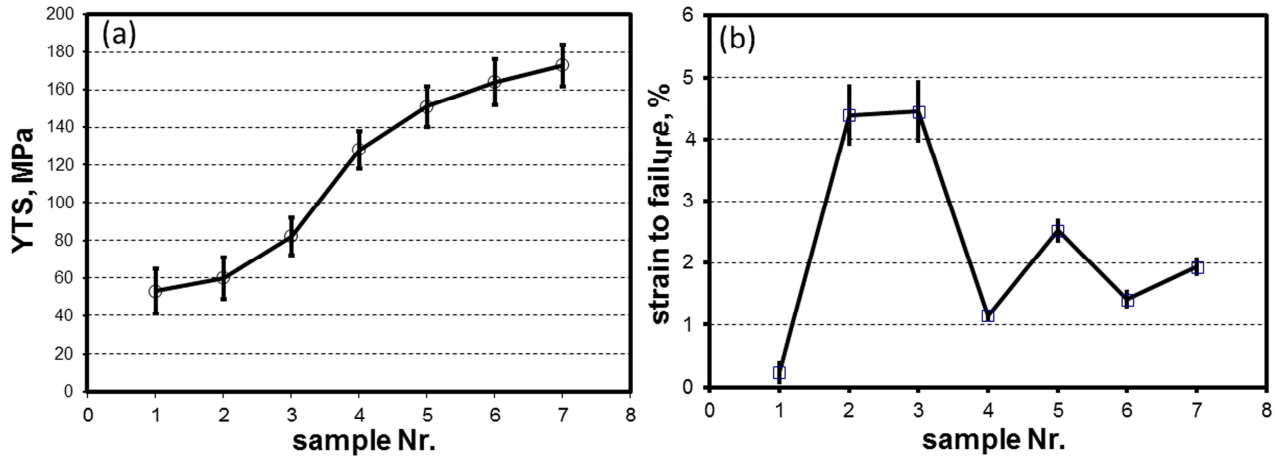

Fig. 7 (a) Tensile yield strength and (b) tensile elongation of S1 to S7.

Table 1 Deformation degree of the swaged samples.

Sample	Diameter, mm	True strain
S1	10.02	0.00
S2	8.60	0.31
S3	6.80	0.78
S4	6.05	1.01
S5	4.90	1.43
S6	4.55	1.58
S7	4.55	1.58